Talanta 93 (2012) 433–438

Contents lists available at SciVerse ScienceDirect

Talanta

journal homepage: www.elsevier.com/locate/talanta

Short communication

Electrochemical immunosensor for competitive detection of neuron specific enolase using functional carbon nanotubes and gold nanoprobe

Tianxiao Yu[a,1], Wei Cheng[a,c,1], Qing Li[a], Caihui Luo[a], Li Yan[a], Decai Zhang[a], Yibing Yin[a], Shijia Ding[a,*], Huangxian Ju[a,b,**]

[a] Key Laboratory of Clinical Laboratory Diagnostics (Ministry of Education), Department of Laboratory Medicine, Chongqing Medical University, Chongqing 400016, China
[b] State Key Laboratory of Analytical Chemistry for Life Science, Department of Chemistry, Nanjing University, Nanjing 210093, China
[c] Molecular Oncology and Epigenetics Laboratory, The First Affiliated Hospital of Chongqing Medical University, Chongqing 400016, China

ARTICLE INFO

Article history:
Received 26 September 2011
Received in revised form 16 February 2012
Accepted 22 February 2012
Available online 1 March 2012

Keywords:
Electrochemical immunosensors
Single-walled carbon nanotubes
Gold nanoparticles
Neuron specific enolase

ABSTRACT

An electrochemical immunosensor for detection of neuron specific enolase (NSE) was designed by immobilizing NSE covalently functionalized single-walled carbon nanotubes (NSE-SWNTs) on a glassy carbon electrode. The NSE-SWNTs not only enhanced electrochemical signal but also presented abundant antigen domains for competitive immunological recognition to anti-NSE primary antibody and then gold nanoprobes labeled with alkaline phosphatase conjugated secondary antibody (AP-anti-IgG/AuNPs). The AP-anti-IgG/AuNPs exhibited highly catalytic activity toward enzyme substrate and significantly amplified the amperometric signal for target molecule detection. Based on the dual signal amplification of SWNTs and gold nanoprobe, the immunosensor could response down to 0.033 ng mL^{-1} NSE with a linear range from 0.1 ng mL^{-1} to 2 μg mL^{-1}, and showed acceptable precision and reproducibility. The designed immunosensor was amenable to direct quantification of target protein with a wide range of concentration in complex clinical serum specimens. The assay results were in a good agreement with the reference values. The proposed electrochemical immunosensor provided a pragmatic platform for convenient detection of tumor markers in clinical diagnosis.

1. Introduction

The quantitative detection of tumor markers in biological specimens plays important roles in screening and diagnosis of cancers [1–3]. Various immunoassay methods have been developed to detect tumor markers in clinical laboratory, including enzyme-linked immunosorbent assay [4,5], radio immunoassay [6], fluorescence immunoassay [7] and chemoluminescence immunoassay [8]. In comparison with these immunological methods, electrochemical immunosensor has attracted considerable interest for its intrinsic advantages such as simple, low cost, good portability, and high sensitivity [9].

To achieve highly sensitive electrochemical immunosensing, various nanomaterials have recently been applied for signal amplification, including gold nanoparticles [10], carbon nanostructures [11–13] and quantum dots [14,15]. All these nanomaterials are excellent carriers in the amplification of recognition events and enhancement of signal transduction [16,17]. As one of the most popular reporter labels, enzymes, including alkaline phosphatase (AP), horseradish peroxidase (HRP) and glucose oxidase (GOD) have been immobilized with primary antibodies on nanomaterials for enhancing the enzymatically catalytical signal [11,18,19]. However, most researches pay primary attention to achieving high sensitivity of the immunosensors, take little account of the ability to detect high-concentration practical samples which are frequent in clinical laboratory diagnosis. For example, neuron specific enolase (NSE), a widely used biomarker for small-cell lung cancer [20], neuroblastoma [21], and neuroendocrine cancers [22], often expresses up to nearly 1 μg mL^{-1} in serum of serious cancer patients [23]. Clinical samples with high-concentration target proteins cannot be directly detected using these electrochemical immunosensors [24,25], and the sample dilution process will result in more complex procedure and an inaccurate result, which limits their practical application in clinical laboratory diagnosis of cancers. Therefore, it remains a challenge to develop a simple, pragmatic, sensitive immunosensor that can also directly detect high concentration cancer markers in clinical specimens.

Herein, using NSE as a model, a novel electrochemical immunosensor was prepared by modifying a glassy carbon

* Corresponding author. Tel.: +86 23 68485688; fax: +86 23 68485786.
** Corresponding author at: Key Laboratory of Clinical Laboratory Diagnostics (Ministry of Education), Department of Laboratory Medicine, Chongqing Medical University, Chongqing 400016, China. Tel.: +86 23 68485688; fax: +86 23 68485786.
E-mail addresses: dingshijia@163.com (S. Ding), hxju@nju.edu.cn (H. Ju).
[1] These authors contributed equally to this work.

0039-9140/$ – see front matter © 2012 Elsevier B.V. All rights reserved.
doi:10.1016/j.talanta.2012.02.047

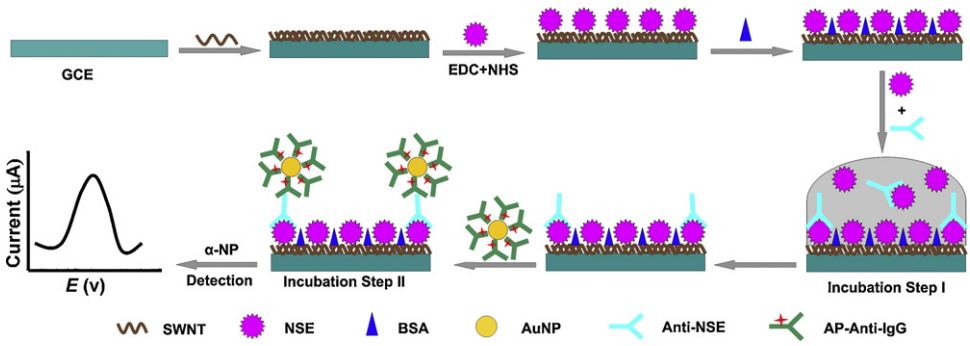

Scheme 1. Schematic representation of the designed electrochemical immunosensor for NSE detection.

electrode (GCE) with NSE covalently functionalized single-walled carbon nanotubes (NSE-SWNTs). The excellent electrical conductivity of SWNTs and the high loading of NSE on SWNTs not only enhanced electrochemical signal but also presented abundant antigen domains for competitive recognition to anti-NSE primary antibody, which greatly extended the up-limit of the detectable range. Using alkaline phosphatase conjugated secondary antibody to label gold nanoparticle, a gold nanoprobe, AP-anti-IgG/AuNP, was designed for immunoassay. The AP-anti-IgG/AuNPs exhibited highly catalytic activity toward hydrolysis of α-naphthyl phosphate (α-NP), leading to a dual signal amplification of SWNTs and gold nanoprobe for detection of low-concentration target (Scheme 1). Meanwhile, in the competitive format the high loading of NSE on SWNTs was sufficiently utilized to greatly extend the up-limit of the detectable range of the designed immunosensor. The proposed method showed low cost, acceptable precision and reproducibility, and could be successfully applied in direct detection of NSE in clinical serum specimens. The designed immunosensor provided a pragmatic tool for convenient detection of tumor markers in clinical diagnosis.

2. Experimental

2.1. Reagents and apparatus

Neuron specific enolase, rabbit anti-NSE polyclonal antibody (1 mg mL^{-1}) and AP-labled goat anti-rabbit antibody (AP-anti-IgG, 1 mg mL^{-1}) were purchased from Beijing Biosynthesis Biotechnology Ltd. Co. (Beijing, China). $HAuCl_4{\cdot}4H_2O$ was purchased from Sinopharm Chem Ltd. Co. (Shanghai, China). Carboxylic group-functionalized SWNTs (<5 nm diameter) were purchased from Shenzhen Nanotech Port Ltd. Co. (Shenzhen, China). Bovine serum albumin (BSA), N-hydroxysuccinimide (NHS), 1-ethyl-3-(3-dimethyllaminopropyl) carbodiimide hydrochloride (EDC) and α-naphthyl phosphate (α-NP) were obtained from Sigma Aldrich (USA). Other reagents were of analytical grade. All aqueous solutions were prepared using 18 MΩ ultrapure water.

The electrochemical measurements were performed on a CHI 660D electrochemical analyzer (Shanghai Chenhua Instrument, China). The electrochemical system consisted of a three-electrode system where a SWNTs-modified GCE (3 mm in diameter) was used as a working electrode, platinum wire was used as an auxiliary electrode, and an Ag/AgCl was used as a reference electrode. UV–visible spectra were carried out on a UV (3150)-Vis spectrophotometer (Jiangsu Jialing Instrument, China). Transmission electron microscopic (TEM) image was taken with an H-7500 transmission electron microscope (Hitachi, Japan).

2.2. Preparation of gold nanoparticle

AuNPs were prepared according to the method reported previously by adding 1 mL of 1% trisodium citrate aqueous solution to 100 mL of boiling 0.01% $HAuCl_4$ deionized water solution [26]. The mixture was maintained at boiling point for 15 min and stirred to cool completely after removing the heating source to produce 24 nm-diameter AuNPs, which were stored at 4 °C. All glassware used in this procedure was cleaned in freshly prepared 1:3 HNO_3–HCl and then rinsed thoroughly in deionized water.

2.3. Preparation of gold nanoprobe

The bioconjugation of the synthesized AuNPs and AP-anti-IgG was prepared according to the literature [27]. 2 mL colloidal AuNP solution was initially adjusted to pH 9.0–9.5 using Na_2CO_3, and then 0.1 mL of the original AP-anti-IgG was added, after incubated for 12 h at 4 °C with slight stirring, the mixture was centrifugated (13,000 rpm) at 4 °C for 30 min, then the obtained AP-anti-IgG/AuNPs conjugates were resuspended into 3.0 mL pH 7.4 PBS. The synthesized gold nanoprobe was stored at 4 °C.

2.4. Preparation of immunosensor

The GCE was polished to a mirror using 0.3 and 0.05 μm alumina slurry followed by rinsing thoroughly with deionized water. After sonicated in 1:1 nitric acid and acetone, the electrode was sonicated again in deionized water, rinsed with deionized water and allowed to dry at room temperature. Then 2 μL of 1 mg mL^{-1} carboxylic group functionalized SWNTs solution was dropped on the pretreated GCE and dried in a desiccator. 10 μL of 4 mM EDC and 10 mM NHS mixed liquor was dropped onto the SWNTs-coated GCE surface and incubated for 1 h to activate the carboxylic group functionalized SWNTs. After the activated SWNTs/GCE was thoroughly rinsed with deionized water, 10 μL of 5 μg mL^{-1} NSE was immediately dropped on its surface and then incubated for 2 h. After rinsed thoroughly with 0.01 M pH 7.4 PBS, the obtained immunosensor was stored at 4 °C prior to electrochemical assays.

2.5. Electrochemical measurements

Firstly, the NSE-SWNTs/GCE was immersed in 1% BSA solution for 30 min to block the nonspecific binding sites on the surface. Then, the immunosensor was immersed in 50 μL incubation solution, which was prepared by mixing 40 μL NSE standard solution or serum sample with 10 μL of 5 μg mL^{-1} anti-NSE primary antibody, for 60 min at 37 °C for competitive immunoreaction (Incubation step I). After the immunosensor was washed carefully with 0.01 M pH 7.4 PBS, 5 μL of AP-anti-IgG/AuNPs was dropped on its surface and incubated at 37 °C for 60 min (Incubation step II). Following a rinse with 0.01 M pH 7.4 PBS, the electrochemical measurement was performed in pH 9.5 DEA solution (0.1 mol L^{-1} diethanolamine, 1 mmol L^{-1} $MgCl_2$, 100 mmol L^{-1} KCl) containing 1.2 mg mL^{-1} α-NP. The differential pulse voltammetric (DPV)

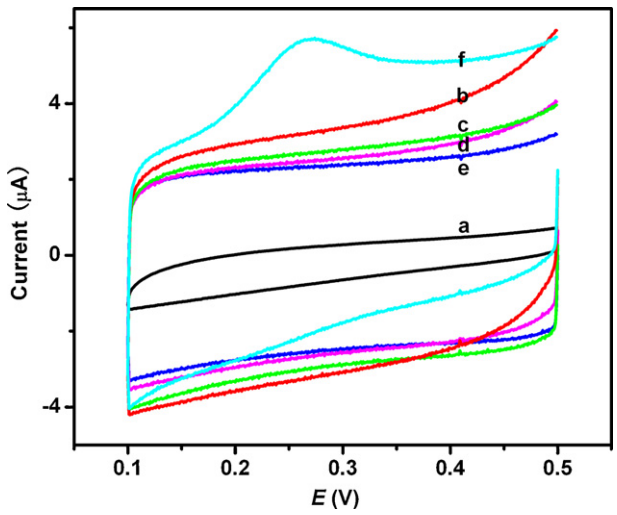

Fig. 1. Cyclic voltammograms of (a) bare GCE, (b) SWNTs/GCE, (c) NSE-SWNTs/GCE, (d) anti-NSE/NSE-SWNTs/GCE, (e) AP-anti-IgG/AuNPs/anti-NSE/NSE-SWNTs/GCE in pH 9.5 DEA, and (f) AP-anti-IgG/AuNPs/anti-NSE/NSE-SWNTs/GCE in pH 9.5 DEA containing 1.2 mg mL^{-1} α-NP. Scan rate: 100 mV s^{-1}.

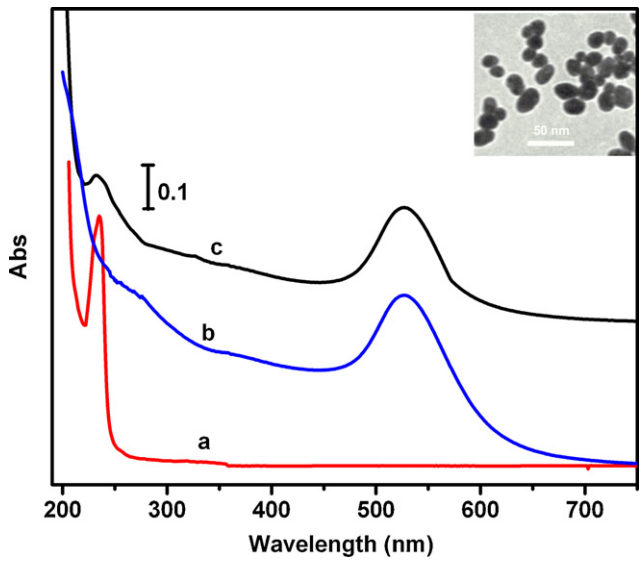

Fig. 2. UV–vis absorption spectra of (a) AP-anti-IgG, (b) AuNPs, and (c) AP-anti-IgG/AuNPs. Inset: TEM image of AuNPs.

measurement was performed from 0 to 0.5 V with pulse amplitude of 50 mV.

3. Results and discussion

3.1. Cyclic voltammetric behavior of modified electrodes

The cyclic voltammograms of GCE, SWNTs/GCE, NSE-SWNTs/GCE, anti-NSE/NSE-SWNTs/GCE, and AP-anti-IgG/AuNPs/anti-NSE/NSE-SWNTs/GCE in pH 9.5 DEA solution did not show any detectable signal (Fig. 1). The presence of SWNTs on the GCE surface resulted in an excessive increase in the background current due to the increased surface area [28]. Upon addition of α-NP in the DEA solution, the cyclic voltammogram of AP-anti-IgG/AuNPs/anti-NSE/NSE-SWNTs/GCE appeared a stable and well-defined oxidation peak at 0.270 V (Fig. 1, curve f), which corresponded to the oxidation of α-naphthyl, the enzymatic hydrolysis product of α-NP [29]. The electrochemical signal was directly related to the amount of the AP-anti-IgG/AuNPs, which depended on the concentration of target antigen in the sample. Thus, quantitative detection of the NSE could be carried out by monitoring the gold nanoprobe-amplified electrochemical signal.

3.2. Characteristics of AP-anti-IgG/AuNPs

TEM image of the prepared AuNPs showed a homogeneous distribution with a mean size of 24 nm in diameter (Fig. 2, inset). The bioconjugation of AP-anti-IgG on the synthesized AuNPs was confirmed by UV–vis absorption spectra (Fig. 2). The AP-anti-IgG solution showed an absorption peak of protein at nearly 260 nm, and the AuNPs exhibited the characteristic absorption peak at about 520 nm. After AP-anti-IgG was loaded on the AuNPs, these two absorption peaks were observed simultaneously, indicating the successful labeling of AuNPs with AP-anti-IgG.

3.3. Optimization conditions for immunoreaction

The incubation time for the competitive immunoreaction (Incubation step I) and the specific binding AP-anti-IgG/AuNPs to anti-NSE antibody (Incubation step II) was optimized. With the increasing incubation time, the DPV peak current sharply increased and tended to a steady value after 60 min, respectively, and longer incubation time did not improve the response (Fig. 3A and B). So 60 min was chosen as the optimal incubation time in incubation step I and II, respectively.

In the competitive immunoreaction, the target NSE competed with the NSE domains on the electrode surface to bind the anti-NSE antibody in the incubation solution. Thus, the amount of anti-NSE antibody in the incubation solution was a key factor in the competitive immunoassay format. In order to obtain the optimal concentration of anti-NSE antibody, NSE-SWNTs/GCEs were incubated in anti-NSE antibody solutions with different concentrations. As shown in Fig. 3C, the peak current increased with the increasing anti-NSE antibody concentration and tended to a plateau at 5 μg mL^{-1}, indicating that all the available recognition sites of immobilized NSE were matched with the anti-NSE antibody. Thus, 5 μg mL^{-1} of anti-NSE antibody was used for the incubation step I.

The effect of dilution of prepared AP-anti-IgG/AuNPs solution in the Incubation step II on the DPV response was shown in Fig. 3D. At high concentrations, the immunosensor showed the maximum response due to the saturated binding, which persisted to the dilution of 1:30 for AP-anti-IgG/AuNPs. Further dilution resulted in the decrease of response of the immunosensor. Thus, the incubation solution was prepared according to the optimal dilution.

3.4. Optimization of conditions for electrochemical detection

The pH of the substrate solution was an important parameter that influenced the enzyme-catalyzed reaction. The pH value was investigated between 8.0 and 10.5, with the maximum response at pH 9.5 (Fig. 4A), that was just the optimum pH value for the maximum activity of AP.

The performance of the electrochemical analysis was related to the concentration of α-NP in the measuring system. The DPV peak current of the immunosensor in DEA increased with the increasing concentration of α-NP from 0.6 to 1.2 mg mL^{-1}, and then tended to a plateau at higher concentrations. Afterward, the enzymatic reaction rate depended on the amount of the AP-anti-IgG/AuNPs binding on the immunosensor. Therefore, the optimal α-NP concentration for gold naoprobe-amplified DPV detection was 1.2 mg mL^{-1} (Fig. 4B).

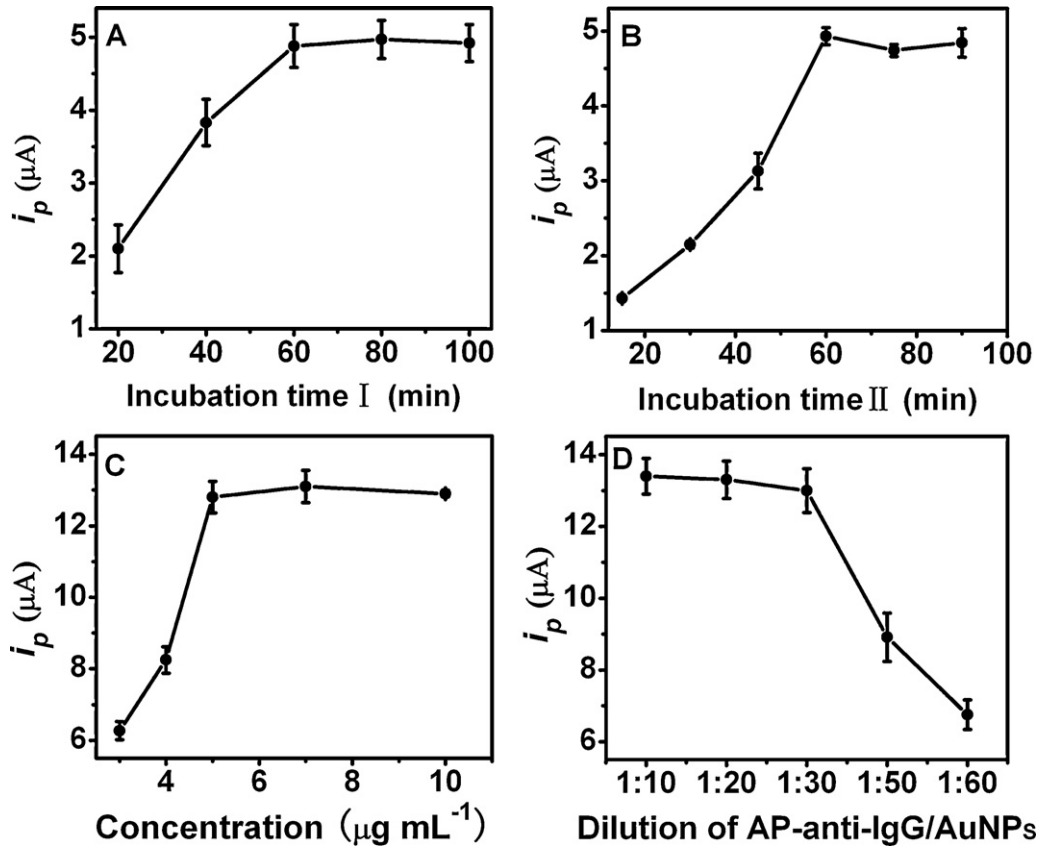

Fig. 3. Dependences of peak current on incubation time of (A) incubation step I and (B) incubation step II at 100 ng mL^{-1} NSE, (C) incubation concentration of anti-NSE and (D) dilution of AP-anti-IgG/AuNP in absence of NSE, when one parameter changes while the others are under their optimal conditions. The error bars represent the standard deviations calculated from three different assays.

3.5. Analytical performance

To clarify the analytical performance of the electrochemical immunosensor using AP-anti-IgG/AuNP as a detection probe, a control method was designed using AP-anti-IgG as detection probe to bind the anti-NSE/NSE-SWNTs/GCE. Different levels of NSE were assayed using the same batch immunosensors and different detection probes, respectively (Fig. 5). In control experiment, the immunosensor was performed through the full procedure without addition of anti-NSE in Incubation step I, which did not behave any conspicuous peak in the detection solution (curves i). However, the DPV signal of blank sample obviously increased to 13.75 μA using AP-anti-IgG/AuNP as a detection probe, comparing with that of 6.42 μA using AP-anti-IgG (curve a). The results proved that the AP-anti-IgG/AuNPs greatly enhanced the signal intensity of the designed immunosensor, and significantly elevated the sensitivity of the immunosensor for NSE detection (Fig. 6).

Under the optimal conditions, the DPV peak current decreased proportionally with the increasing logarithm value of NSE concentration (Fig. 5A). The linear response was over a range from 0.1 ng mL^{-1} to 2 μg mL^{-1} with a correlation coefficient of 0.997 (Fig. 6a). The upper limit of linear response was

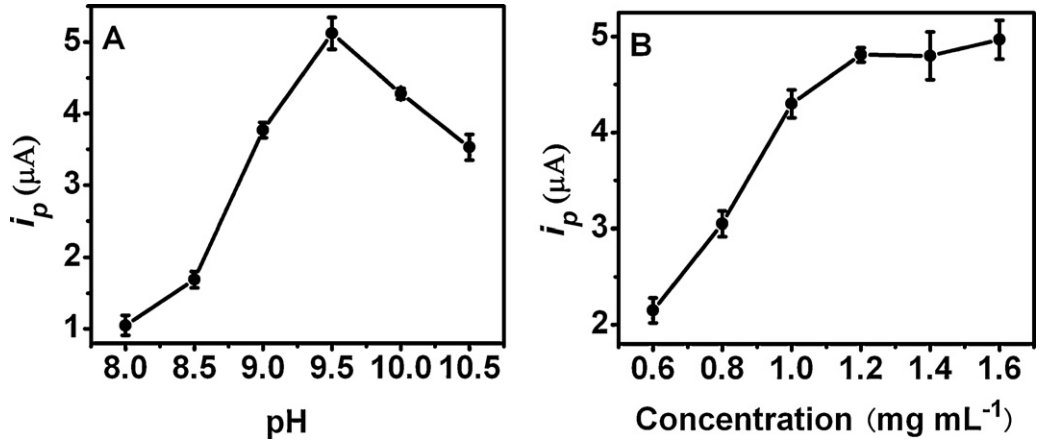

Fig. 4. Dependences of peak current on (A) pH of detection solution and (B) concentration of α-NP at 100 ng mL^{-1} NSE. The error bars represent the standard deviations calculated from three different assays.

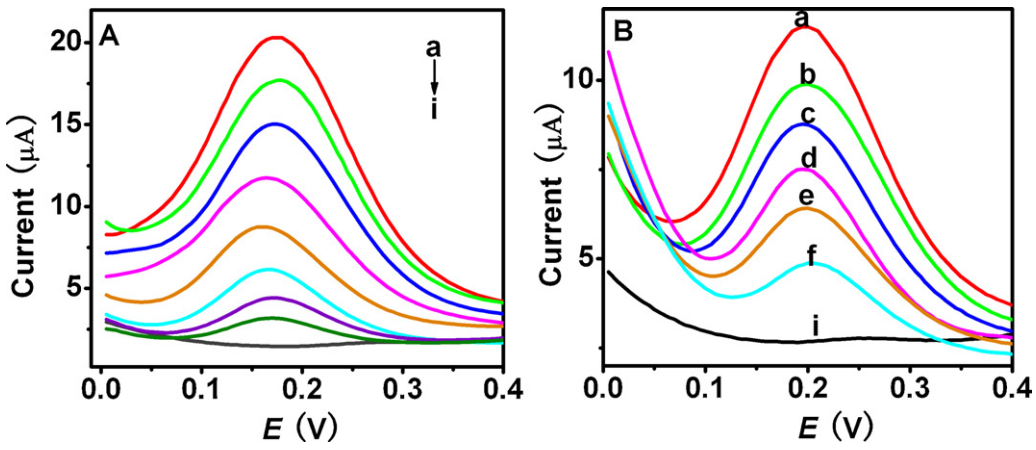

Fig. 5. Typical DPV curves of (A) AP-anti-IgG/AuNP/anti-NSE/NSE-SWNTs/GCE and (B) AP-anti-IgG/anti-NSE/NSE-SWNTs/GCE obtained at 0, 0.1, 1, 10, 100, 5×10^2, 1×10^3, 2×10^3 ng mL^{-1} NSE and control without anti-NSE (from a to i).

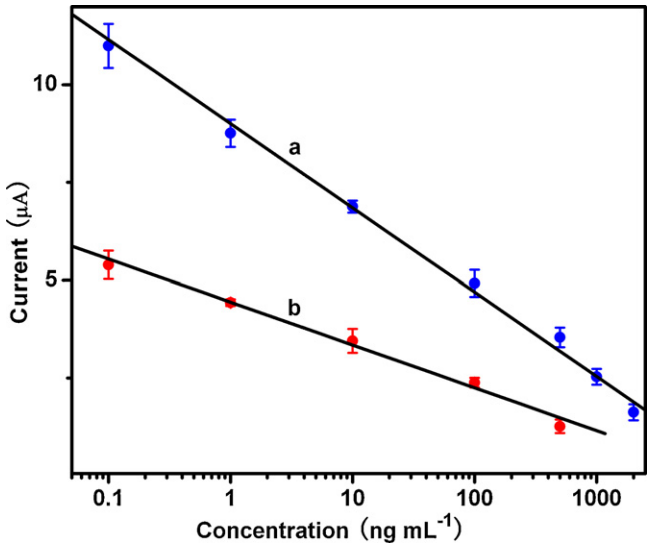

Fig. 6. Plots of peak current versus the logarithm of NSE concentration of using (a) AP-anti-IgG/AuNP and (b) AP-anti-IgG as detection probe. The error bars represent the standard deviations calculated from three different assays.

much higher than those of 120 ng mL^{-1} prostate-specific antigen (PSA) for electrochemical immunoassay using HRP labled anti-PSA [19], 200 ng mL^{-1} tumor necrosis factor (TNF) for electrochemical immunosensor based on AP functionalized nanosphere [18], 500 ng mL^{-1} alpha-fetoprotein (AFP) for conductometric immunoassay using carbon nanoparticles (CNP) as labels [11]. The limit of detection (LOD) was calculated to be 0.033 ng mL^{-1} by four-parameter logistic equation, which was much lower than clinical decision level of 12.5 ng mL^{-1} [30]. To further highlight the merits of the designed electrochemical immunosensor, the analytical properties were compared with those of other sensors [31–35]. Characteristics including the linear range and LOD are summarized in Table 1. It proved that the immunosensor not only had high sensitivity but also possessed the advantage to detect high-concentration biomarkers. Thus, the proposed method was competent for direct quantification of target protein with a wide range of concentration in complex clinical serum specimens.

The intra-assay precision of the proposed method was further evaluated by five replicative measurements of NSE at two levels with the same batch of immunosensors. The intra-assay variation coefficients were 3.27% and 6.64% at NSE concentrations of 10 ng mL^{-1} and 1 μg mL^{-1}, respectively, showing a good repeatability. While the inter-assay variation coefficients for five batches of immunosensors at these concentrations were 6.14% and 8.18%, respectively, indicating acceptable fabrication reproducibility.

3.6. Application of in analysis of clinical serum samples

The feasibility of the designed immunosensor in clinical laboratory diagnosis was investigated by analyzing 16 clinical serum specimens, and comparing with the electrochemiluminescent method (Roche 2010 Electrochemiluminescent Automatic Analyzer). The comparison between the results of the proposed immunosensor and the reference method was shown in Table 2. The relative standard deviations of the two methods were from 1.0% to 6.7%, indicating no significant difference between the results given by two methods. Since there is no any pretreatment for the serum specimens, the matrix interfering effect on the immunoassay can be neglected and the selectivity of the immunosensor was acceptable. The immunosensor, which is distinguished by its convenient miniaturization for low assay cost, high sensitivity, and absence of sophisticated and expensive array detectors, shows more suitable for point-of-care testing. Therefore, the developed immunosensor

Table 1
Comparison of analytical performance of the proposed electrochemical immunosensor with that of reported immunosensors for detection of tumor marker.

Fabrication[a]	Methods	Dynamic range (ng mL^{-1})	Detection limit (ng mL^{-1})	Ref.
HRP-P4/Anti-P4/GCE	Microfluidic immunosensor	0.50–12.5	0.20	[31]
Ru(bpy)32+-Si-anti-AFP/AFP/anti-AFP/MUA/GE	Electrochemiluminescence immunosensor	0.05–30	0.035	[32]
FITC-anti-IgM/IgM/anti-IgM/eggshell membrane	Fluorescence immunosensor	5–60	4.30	[33]
HRP-anti-AFP/AFP/anti-AFP/AuNPs/CPE	Electrochemical immunosensor	0.50–80	0.25	[34]
CEA/anti-CEA/CNTs–AuNPs/GCE	Electrochemical immunosensor	0.10–200	0.04	[35]
AP-anti-IgG/AuNPs/anti-NSE/NSE-SWNTs/GCE	Electrochemical immunosensor	0.10–2000	0.03	This work

[a] SCE: saturated calomel electrode; P4: progesterone; CPE: carbon paste electrode; MUA: 11-mercapto-1-undecanoic acid; FITC: fluorescein isothiocyanate.

Table 2
Assay results of clinical serum samples using the proposed electrochemical immunosensor and reference method. Each sample was assayed in triplicate (mean ± SD).

Sample no.	Electrochemiluminescent ($ng\,mL^{-1}$)	[a]Immunosensor ($ng\,mL^{-1}$)	Mean ± SD	RSD%
1	10.69	10.92	10.805 ± 0.16	1.5
2	19.36	20.41	19.885 ± 0.74	3.7
3	9.73	9.51	9.62 ± 0.16	1.6
4	3.87	3.95	3.91 ± 0.06	1.4
5	6.38	6.48	6.43 ± 0.07	1.1
6	14.13	13.93	14.03 ± 0.14	1.0
7	7.53	7.73	7.63 ± 0.14	1.9
8	117.7	120.23	118.97 ± 1.79	1.5
9	12.04	12.32	12.18 ± 0.20	1.6
10	13.29	13.59	13.44 ± 0.21	1.6
11	7.60	7.42	7.51 ± 0.13	1.7
12	6.98	7.10	7.04 ± 0.08	1.2
13	66.46	69.18	67.82 ± 1.9	2.8
14	21.46	19.50	20.48 ± 1.39	6.7
15	21.91	22.39	22.15 ± 0.34	1.5
16	8.22	8.38	8.3 ± 0.11	1.4

[a] The average of three successful assays.

could be potential tool for convenient detection of NSE in serum specimens in clinical laboratory diagnosis.

4. Conclusions

A versatile electrochemical immunosensor is developed for detection of NSE in serum specimens with NSE-SWNTs modified GCE by using AP-anti-IgG/AuNP as a nanoprobe. NSE-SWNTs can offer abundant antigen domains for competitive immunoassay and the AP-anti-IgG/AuNPs exhibit highly catalytic activity toward hydrolysis of α-NP, producing a strategy of dual signal amplification for detection of target protein. With a competitive immunoassay format, the designed immunosensor for NSE shows good performance with high sensitivity, a wide linear range, acceptable precision and fabrication reproducibility. It has been successfully applied in the direct detection of NSE in practical serum specimens. The developed electrochemical immunosensor would become a pragmatic tool for convenient detection of NSE in clinical laboratory diagnosis and could be easily extended to detection of other protein cancer markers for clinical screening of cancers.

Acknowledgment

This work was supported by the National Natural Science Foundation of China (21075141).

References

[1] R.G. Moore, S.M. Laughlan, R.C. Bast Jr., Gynecol. Oncol. 116 (2010) 240–245.
[2] S.F. Shariat, Y. Lotan, A. Vickers, P.I. Karakiewicz, B.J. Schmitz-Dräger, P.J. Goebell, N. Malats, Urol. Oncol. Semin. Orig. 28 (2010) 389–400.
[3] V.V. Levenson, BBA Gen. Subj. 1770 (2007) 847–856.
[4] L.S. Zhao, S.Y. Xu, G. Fjaertoft, K. Pauksen, L. Hakansson, P. Venge, J. Immunol. Methods 293 (2004) 207–214.
[5] T. Tagi, T. Matsui, S. Kikuchi, S. Hoshi, T. Ochiai, Y. Kokuba, Y. Kinoshita-Ida, F. Kisumi-Hayashi, K. Morimoto, T. Imai, I. Imoto, J. Inazawa, E. Otsuji, J. Gastroenterol. 45 (2010) 1201–1211.
[6] Q.Y. Zhang, Q. Xiao, Z. Lin, X. Ying, Zh.J. Li, J.M. Lin, Clin. Biochem. 43 (2010) 1003–1008.
[7] S.W. Oh, Y.M. Kim, H.J. Kim, S.J. Kim, J.S. Cho, E.Y. Choi, Chim. Clin. Acta 406 (2009) 18–22.
[8] X. Wang, Q.Y. Zhang, Zh.J. Li, X.T. Ying, J.M. Lin, Clin. Chim. Acta 393 (2008) 90–94.
[9] J.H. Lin, H.X. Ju, Biosens. Bioelectron. 20 (2005) 1461–1470.
[10] R. Chai, R. Yuan, Y.Q. Chai, C.F. Ou, S.R. Cao, X.L. Li, Talanta 74 (2008) 1330–1336.
[11] J. Tang, J.X. Huang, B.L. Su, H.F. Chen, D.P. Tang, Biochem. Eng. J. 53 (2011) 223–228.
[12] W. Cheng, L. Ding, J.P. Lei, S.J. Ding, H.X. Ju, Anal. Chem. 80 (2008) 3867–3872.
[13] D. Wen, X.Q. Zou, Y. Liu, L. Shang, S.J. Dong, Talanta 79 (2009) 1233–1237.
[14] K. Pinwattana, J. Wang, C.T. Lin, H. Wu, D. Du, Y.H. Lin, O. Chailapaku, Biosens. Bioelectron. 26 (2010) 1109–1113.
[15] X. Liu, Y.Y. Zhang, J.P. Lei, Y.D. Xue, L.X. Cheng, H.X. Ju, Anal. Chem. 82 (2010) 7351–7356.
[16] D.P. Tang, J. Tang, B.L. Su, G.N. Chen, Biosens. Bioelectron. 26 (2011) 2090–2096.
[17] A. Umar, M.M. Rahman, A. Al-Hajry, Y.B. Hahn, Talanta 78 (2009) 284–289.
[18] Z.Z. Yin, Y. Liu, L.P. Jiang, J.J. Zhu, Biosens. Bioelectron. 26 (2011) 1890–1894.
[19] S.Q. Liu, X.T. Zhang, Y.F. Wu, Y.F. Tu, L. He, Clin. Chim. Acta 395 (2008) 51–56.
[20] T. Hirose, K. Okuda, T. Yamaoka, K. Ishida, S. Kusumoto, T. Sugiyama, T. Shirai, T. Ohnshi, T. Ohmori, M. Adachi, Lung Cancer 71 (2011) 224–228.
[21] S.T. Bolkar, M.S. Ghadge, A.S. Raste, Ind. J. Clin. Biochem. 23 (2008) 293–295.
[22] A. Komiya, H. Suzuki, T. Imamoto, N. Kamiya, N. Nihei, Y. Naya, T. Ichikawa, H. Fuse, Int. J. Urol. 16 (2009) 37–44.
[23] M. Harding, J. McAllister, G. Hulks, D. Vernon, R. Monie, J. Paul, S.B. Kaye, Br. J. Cancer 61 (1990) 605–607.
[24] J. Tang, D.P. Tang, Q.F. Li, B.L. Su, B. Qiu, G.N. Chen, Anal. Chim. Acta 697 (2011) 16–22.
[25] F. Yan, J. Wu, F. Tan, Y.T. Yan, H.X. Ju, Anal. Chim. Acta 644 (2009) 36–41.
[26] D.P. Tang, R. Yuan, Y.Q. Chai, Anal. Chim. Acta 564 (2006) 158–165.
[27] J. Tang, B.L. Su, D.P. Tang, G.N. Chen, Biosens. Bioelectron. 25 (2010) 2657–2662.
[28] H.X. Luo, Z.J. Shi, N.Q. Li, Z.N. Gu, Q.K. Zhuang, Anal. Chem. 73 (2001) 915–920.
[29] G. Carpini, F. Lucarelli, G. Marrazza, M. Mascini, Biosens. Bioelectron. 20 (2004) 167–175.
[30] I.E. Tothill, Semin. Cell Dev. Biol. 20 (2009) 55–62.
[31] F.J. Arévalo, G.A. Messina, P.G. Molina, M.A. Zón, J. Raba, H. Fernández, Talanta 80 (2010) 1986–1992.
[32] J. Qian, Zh.X. Zhou, X.D. Cao, S.Q. Liu, Anal. Chim. Acta 665 (2010) 32–38.
[33] J.L. Tang, L. Han, Y.H. Yu, J. Kang, Y.H. Zhang, J. Fluoresc. 21 (2011) 339–346.
[34] C.F. Ding, F. Zhao, R. Ren, J.M. Lin, Talanta 78 (2009) 1148–1154.
[35] X. Gao, Y.M. Zhang, Q. Wu, H. Chen, Z.C. Chen, X.F. Lin, Talanta 85 (2011) 1980–1985.